J. Fluid Mech. (1968), *vol.* 33, *part* 3, *pp.* 457–463
Printed in Great Britain

Finite amplitude convection with changing mean temperature. Part 2. An experimental test of the theory

By RUBY KRISHNAMURTI

Institute of Geophysics and Planetary Physics,
University of California, Los Angeles, California†

(Received 17 August 1967 and in revised form 26 December 1967)

It has been found in part 1 (Krishnamurti 1968) that when the mean temperature of a fluid layer is changing at a constant rate η, hexagonal flows are stable in a range of Rayleigh numbers near the critical. The direction of flow depends upon the sign of η. The static state is unstable to finite amplitude disturbances at Rayleigh numbers below the critical point predicted by linear theory.

The validity of this theory is tested in an experiment in which the heat flux is measured as a function of η and Rayleigh number. The horizontal plan form is determined from the side by continuously exposing a photographic film moving in a vertical direction as tracers in different regions of the fluid are illuminated. Finite amplitude instability and hexagonal cells are indeed observed.

1. Critical observables of the theory

It is known that when a horizontal layer of fluid has an adverse temperature gradient maintained across it, there is an infinitely degenerate set of possible flows at the critical point. It is also known (Schlüter, Lortz & Busse, 1965) that within the Boussinesq approximation and with constant mean temperature the two-dimensional roll is the only stable solution. In part 1 of this study it has been shown that the asymmetry of the temperature profile when the mean temperature is changing at a rate η gives rise to stable hexagonal flows for a range of Rayleigh numbers near the critical. The direction of flow at the centre of the hexagon is downward if η is positive and upward if η is negative. The static state is unstable to finite amplitude disturbances below the linearly predicted critical Rayleigh number.

In a laboratory experiment, the occurrence of hexagons for a range of Rayleigh numbers near critical when other causes for their selection are absent, and the dependence of the direction of flow upon the sign of η are probably the best qualitative tests of the theory.

For η sufficiently large a hysteresis in the heat flux should be measurable when the critical Rayleigh number R_c is approached from below and from above. Based upon rigid boundary calculations from part 1 (and taking infinite Prandtl

† Present address: Institute of Geophysical Fluid Dynamics, Florida State University, Tallahassee, Florida 32306.

number), the difference ΔH in heat flux at R_c is $\Delta H = 16{\cdot}3\eta^2$ where $\eta = (d^2/\kappa\Delta T)(\partial\overline{T}/\partial t)$. For a measurable ΔH, say $\Delta H/H \simeq 25\,\%$, $\eta \simeq 5$ is needed and is easily obtainable. For a quantitative test of the theory the measured heat flux should be extrapolated to small η and amplitude ϵ.

2. Design of an experiment to measure effective conductivity

The validity of the theory can be tested by measuring relative conductivities and relative Rayleigh numbers. For example, the critical Rayleigh number will be measured relative to that for $\eta = 0$. The design in figure 1, similar to the quasi-steady experiment designed by Malkus (1954), allows one to scan slowly through Rayleigh numbers near the critical value.

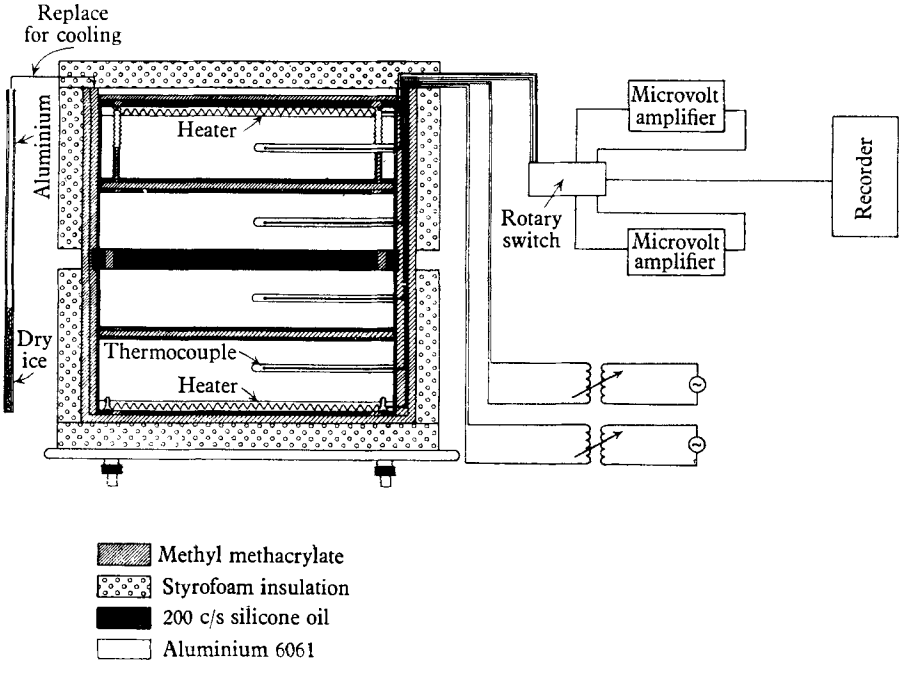

FIGURE 1. The apparatus for measuring heat flux.

The convecting layer is 30 cm by 30 cm by 2 cm in depth of Dow Corning '200 fluid' silicone oil, AA 5871, with kinematic viscosity ν of 200 centistokes. Their variation of viscosity and conductivity k with temperature is relatively small:

$$\frac{1}{\nu}\frac{\partial\nu}{\partial T} \simeq 1\,\%\text{ per °C} \quad \text{and} \quad \frac{1}{k}\frac{\partial k}{\partial T} \simeq 0{\cdot}05\,\%\text{ per °C}.$$

Bounding the convecting layer are four blocks of aluminium 6061 whose thermal diffusivity κ is $0{\cdot}87\ \text{cm}^2\,\text{sec}^{-1}$. For the oil, κ is $1{\cdot}1 \times 10^{-3}\ \text{cm}^2\,\text{sec}^{-1}$. By attempting to approach the perfectly conducting boundary condition of the theory, it follows that temperature gradients in the aluminium are too small to measure. Most of the gradient is across the plastic barrier. The heat flux, and the effective conductivity of the liquid, is determined in terms of the heat flux across this

barrier. The temperature in each of the four aluminum blocks was measured once every minute and a least squares fit to a fourth-order polynomial in time was obtained. This allowed calculation of time derivatives of temperatures. The effective conductivity of the convecting liquid is then obtained in terms of the four temperatures, their time derivatives, the barrier depth and conductivity (Krishnamurti 1967).

2.1. *Precision of the experiment*

By devising a switching arrangement so that both large (around 10 °C) and small (around 0·5 °C) temperature differences appeared as full scale on the recorder, the relative conductivity could be determined to a precision of $\pm 3\,\%$.

2.2. *Accuracy of the experiment*

Since the experiment cannot be performed under the idealized conditions of the theory, each non-ideal condition must be shown not to have a dominating effect.

Non-Boussinesq effects can be shown to be not the reason for realization of hexagons. For the silicone oil

$$\eta_\nu \equiv \frac{1}{\nu}\frac{\partial \nu}{\partial T} = 1\,\% \text{ per } ^\circ\text{C},$$

giving $\eta_\nu R^{(1,1)} = 0{\cdot}1$ (from Busse's (1962) calculation). The corresponding value for changing mean temperature is $\eta R^{(1,1)} = 6\eta$. For $\eta = 8$ this effect is 500 times larger than that due to variation of ν with temperature. Furthermore, a reversal of the direction of flow can be obtained with this effect for any given fluid.

A slow variation of temperature difference ΔT with time has been shown neither to give rise to finite amplitude instability nor to removal of degeneracy (Krishnamurti 1967). As a check, a few data points are obtained with ΔT and η held constant.

The fringing of the isotherms at the lateral boundaries always gives rise to a horizontal component of temperature gradient which drives subcritical rolls at the boundary. However, hexagons or rolls could be formed in a comparatively large area inside these boundary rolls.

Effects such as heat loss, side walls, and finite conductivity of the aluminum upon the heat flux are not important since this is a relative measurement.

A spurious hysteresis in the heat flux due to change of material properties with mean temperature was avoided by comparing results of two experiments at the same mean temperature and Rayleigh number.

3. A method of photographing the plan form when the flow is visible only in elevation

Which plan form would occur near the critical Rayleigh number had been an unanswered question for many decades. Bénard's regular hexagons were shown (Pearson 1958) to be not buoyancy-driven but due to surface tension variation with temperature. Non-linear studies proved rolls to be stable or with variation of material properties, hexagons to be stable. It is noted that Silveston's (1958) three-dimensional cells may not be due to material property variation. Using

a silicone oil with very small η_v his photographs show three-dimensional cells persisting to higher Rayleigh number, the larger the depth d of the layer. Effects of material property variation, on the other hand, would decrease with increased d since then ΔT must be decreased to obtain the same Rayleigh number.

Even with highly conducting opaque boundaries above and below, the plan form can be determined as follows: in figure 2 we let x be in the direction of the optic axis, y normal to the plane of the page, and z in the vertical direction. A narrow collimated beam of light was shone in the y direction, another identical beam in the $-y$ direction so they overlapped. This was for the purpose of visualizing shear regions at positive and negative angles from the line of sight. As the two beams were moved together, the camera was moved horizontally to keep the illuminated region in focus. At the same time the camera was rocked about an axis through its lens thus exposing different parts of the film as different regions of the fluid were illuminated. In this way, photographs were obtained from the side as if one were looking from above. Aluminium flakes were used as tracers.

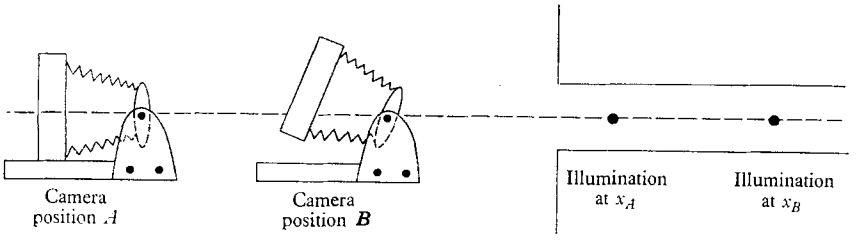

FIGURE 2. Geometry for photographing the plan form of convection.

4. Observations and discussion of results

Figure 3 (*a*), plate 1, shows a static state, 3 (*b*), plate 1, shows roll convection at Rayleigh number just above critical and $\eta = 0$. Figure 3 (*c*), plate 1, shows hexagonal cells obtained under identical conditions as for 3 (*b*), that is, the same apparatus, same fluid, same ΔT, but with the mean temperature changing at a rate of 3·6 °C per hour. Figure 4 (*a*), plate 2, shows hexagonal cells over most of the layer with roll cells along the edge of the layer. It is to be noted that all six sides will not appear bright; the sides which are at 60° or 120° to the line of sight will be relatively bright but the side perpendicular to the line of sight appears dark. Figures 4 (*b*) and (*c*), plate 2, show a transition from hexagonal to roll plan form. Figure 5 (*a*), plate 3, shows 'rolls' as they formed in the square container. Rolls always started in this square array but never remained in this pattern for many hours. Figure 5 (*b*), plate 3, taken about 6 h after the initiation of convection shows the tendency to two-dimensional rolls which end right at the container wall in the upper part of the photograph. In repetitions of the same experiment, the rolls were found after many hours of convection to lie along either of the two perpendicular directions, and occasionally along the diagonal of the container. Figure 5 (*c*), plate 3, photographed after 36 h of convection, shows most of the layer with two-dimensional rolls.

By observing individual aluminium particles by eye, it was confirmed that when η is positive, the motion is upward along the sides of the hexagon and down in the centre. Furthermore, the reverse direction of flow was found for η negative.

The cell size can be easily determined from the photographs. It is found to be a few percent larger than that predicted to correspond to the critical Rayleigh number.

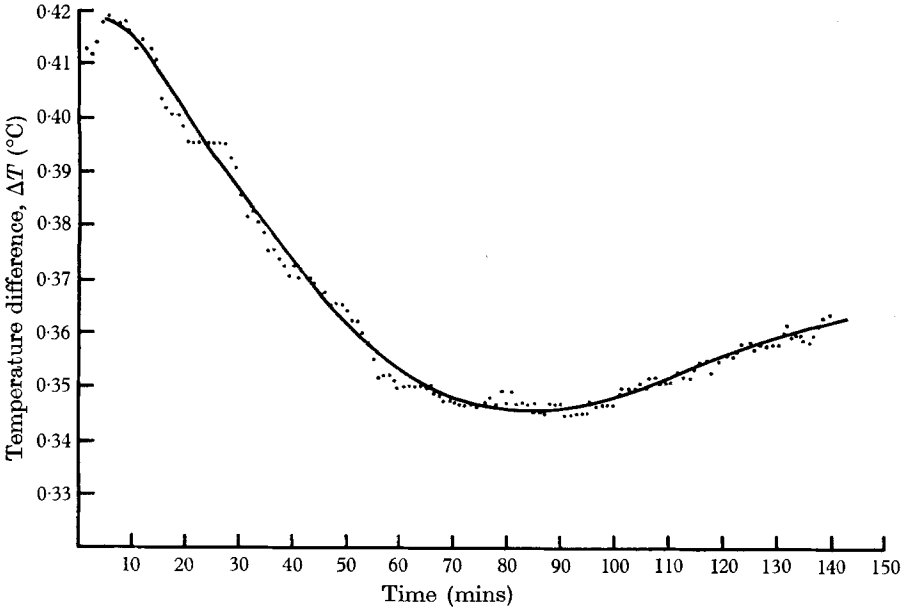

FIGURE 6. The unsmoothed thermocouple output ΔT as a function of time.

A sample of raw data is shown in figure 6 showing a scatter of a few thousandths of a degree. The heat flux H, defined as $H = k_{\text{eff}}\Delta T/d$ where k_{eff} is an effective conductivity of the liquid, is computed as described in §2 and is plotted against ΔT in figure 7. The curve labelled I is for $\eta = 0$ and convection in roll plan form. For sufficiently small ΔT the curve is a straight line whose slope is k/d; the measured slope gives $k = 3{\cdot}7 \times 10^{-4}$ c.g.s. units in agreement to two significant figures to that given by the manufacturer. The critical temperature difference is taken to be that point at which the heat flux curve departs from the conduction curve. This gives $\Delta T_c = 0{\cdot}56\,^{\circ}\text{C}$ in good agreement with a $\Delta T_c = 0{\cdot}53\,^{\circ}\text{C}$ predicted simply by using the manufacturer's listed values of α, κ and ν.

The curved part of the heat flux graph just beyond ΔT_c represents growth of the flow. The points are 1 min apart in time. The slope of the straight portion beyond this is a direct measure of the theoretically predicted $N_0/R^{(2,0)}$. In dimensional form the measured slope is $7{\cdot}4 \times 10^{-4}$ cal sec^{-1} cm^{-2} °C^{-1} in agreement within 6 % with the predicted value. The curve II in figure 7 is one for which the temperature difference was slowly increased with the mean temperature changing at the rate $3{\cdot}6\,^{\circ}$/hour, corresponding to a dimensionless $\eta = 10$. The critical Rayleigh number predicted for $\eta = 10$ is 1465, which is 14 % below the critical number for $\eta = 0$. The observed critical temperature difference is, however, about 40 %

below the critical point for $\eta = 0$. This is interpreted as a finite amplitude instability occurring at a Rayleigh number below that predicted by linear theory. The curve labelled III is one in which ΔT decreased with time, starting with a large value of η which also gradually decreased with time. The oscillation in the heat flux is understood as follows. A convecting fluid can transport heat to its upper boundary, thereby warming it and decreasing ΔT. Depending upon the quantities controlled at the boundary, ΔT may decrease to the point such that convection is no longer sustained. However, if heat is being supplied from below,

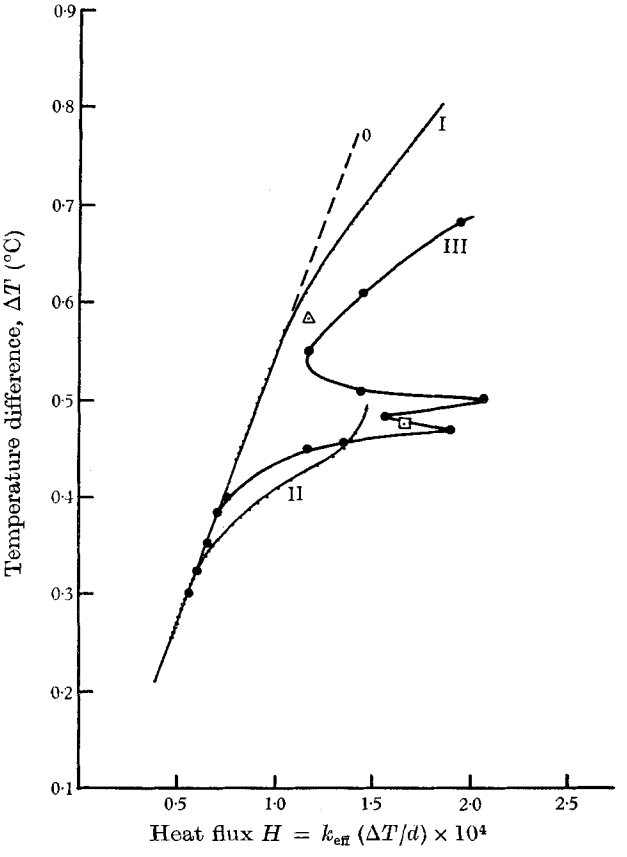

FIGURE 7. Heat flux plotted against temperature difference.

the temperature difference will build up again. When the critical ΔT is reached, convection will start again. Such an oscillatory convection has been studied by Busse (1967) in which he treats the problem of fixed heat flux. Here there is a range of heat flux for which there exists no stable stationary solution. Hours after all heaters were turned off an oscillation in the temperature difference ΔT is directly seen in the unsmoothed thermocouple output (figure 6). The period of oscillation is about 2 h.

Figure 7 also shows two points obtained with constant η and ΔT. The point labelled by a triangle corresponds to $\partial T/\partial t = 2{\cdot}1\,^\circ\text{C/h}$ or $\eta = 3{\cdot}6$. The point labelled by a square corresponds to $\partial T/\partial t = 3{\cdot}1\,^\circ\text{C/h}$ or $\eta = 6{\cdot}7$.

It was seen from the theory that the width of the hysteresis gap, for example, determined by $R^{(1,1)}$ was too small to measure for $\eta < 1$ but sufficiently large for η about 5 or 10. This part of the measurement is not meant to be a quantitative test of the calculation, but the fact that with a large value of η, a greatly increased heat flux is obtained below the linearly predicted critical point is of considerable interest. Nevertheless, the width of the gap and the point of instability are in reasonable agreement with the values computed from the truncated expressions.

5. Conclusions

When the mean temperature was held constant ($\partial\overline{T}/\partial t \lesssim 5 \times 10^{-2}$ °C per hour or $\eta \lesssim 0{\cdot}1$) two-dimensional rolls were found to be the experimentally realized flow pattern near the critical Rayleigh number. With the same fluid under identical conditions, except with the mean temperature changing at a rate of a few degrees per hour ($\eta \simeq 10$), hexagonal cells were found to be the realized flow. The direction of flow at the centre of the hexagon was observed to be downward for η positive and upward for η negative. In spite of opaque boundaries above and below the convecting layer, the 'plan form' was obtained by viewing the layer from the side. Measurements of the heat flux indicate a finite amplitude instability and a hysteresis effect.

This paper is extracted from a Ph.D. dissertation, University of California, at Los Angeles. I am deeply grateful to Professor W. V. R. Malkus for suggesting this problem and for his continued guidance. I also wish to acknowledge the competent work of Mr Paul Cox in building the apparatus, and to thank him for his freely given assistance. The research was supported by the National Science Foundation under Grant GP-2414.

REFERENCES

Busse, F. H. 1962 Dissertation, University of Munich, 1962. Translation from German by S. H. Davis, The RAND Corporation, Santa Monica, California, 1966.

Busse, F. H. 1967 *J. Fluid Mech.* **28**, 223.

Krishnamurti, R. 1967 Dissertation, University of California at Los Angeles.

Krishnamurti, R. 1968 *J. Fluid Mech.* **33**, 445.

Malkus, W. V. R. 1954 *Proc. Roy. Soc.* A **225**, 185.

Palm, E. 1960 *J. Fluid Mech.* **8**, 183.

Palm, E. & Øiann, H. 1964 *J. Fluid Mech.* **19**, 353.

Pearson, J. R. A. 1958 *J. Fluid Mech.* **4**, 489.

Schlüter, A., Lortz, D. & Busse, F. 1965 *J. Fluid Mech.* **23**, 129.

Segel, L. A. & Stuart, J. T. 1962 *J. Fluid Mech.* **13**, 289.

Silveston, P. L. 1958 *Forsch. Ing. Wes.* **24**, 29, 59.

Tippelskirch, H. 1956 *Beiträge zur Physik der Atmosphäre*, **29**, 37.

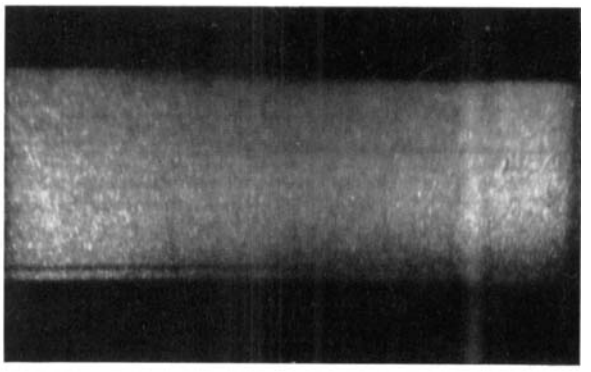

(*a*)

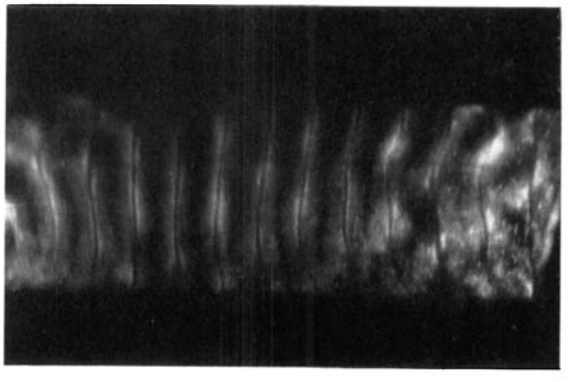

(*b*)

(*c*)

FIGURE 3. A 'plan view' of a layer of liquid. Dow Corning '200' series silicone oil, viscosity 200 cS, conductivity $3{\cdot}7 \times 10^{-4}$ c.g.s., depth 2·0 cm. (*a*) Static state, $\Delta T = 0$, $\eta = 0$. (*b*) Convection in roll plan form, $\Delta T = 0{\cdot}60$ °C, $\eta = 0$. (*c*) Convection in hexagonal plan form, $\Delta T = 0{\cdot}60$ °C, $\eta = 3{\cdot}6°/\text{h}$.

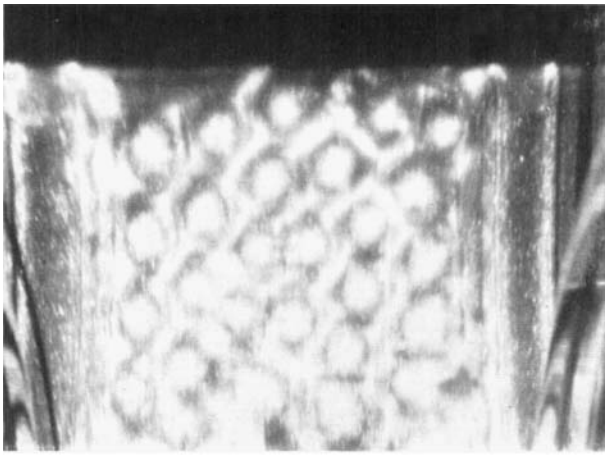

(*a*)

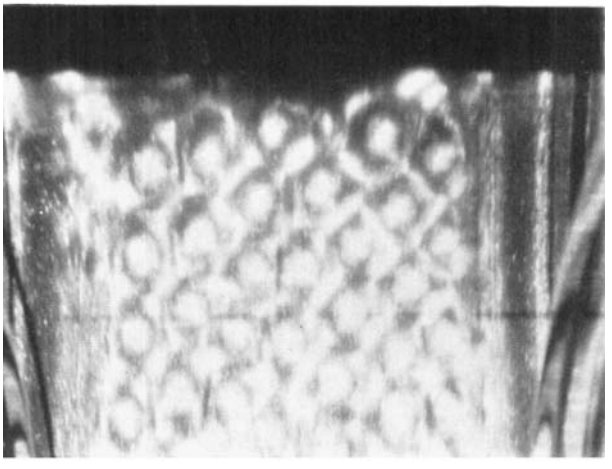

(*b*)

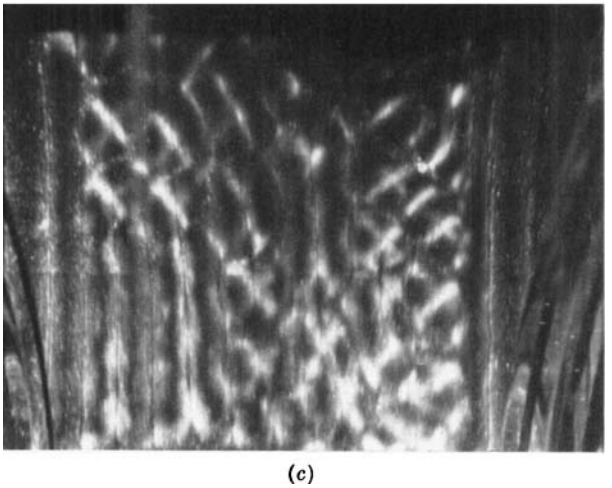

(*c*)

FIGURE 4. A 'plan view' of a layer of liquid in a sequence showing a transition from hexagons to rolls. Dow Corning '200' series silicone oil, viscosity 200 cS, conductivity $3{\cdot}7 \times 10^{-4}$ c.g.s., depth 2·0 cm. (*a*) $\Delta T = 0{\cdot}45$ °C, $\eta = 3{\cdot}0$ °C/h. (*b*) $\Delta T = 0{\cdot}52$ °C, $\eta = 3{\cdot}0$ °C/h. (*c*) $\Delta T = 0{\cdot}69$ °C, $\eta = 2$ °C/h.

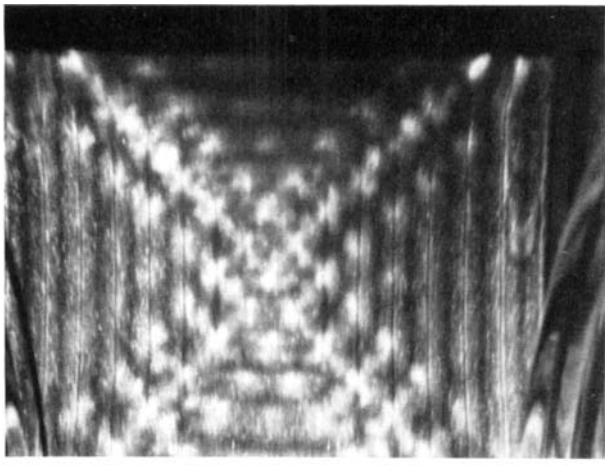

(*a*)

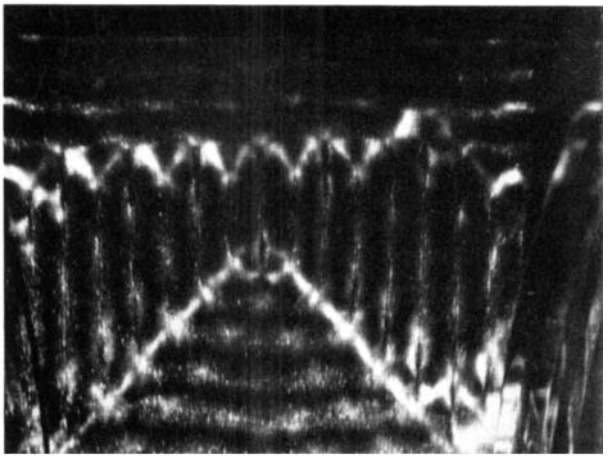

(*b*)

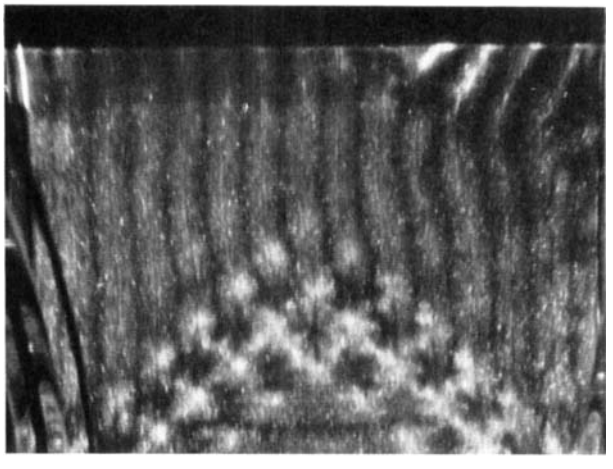

(*c*)

FIGURE 5. A 'plan view' of a layer of liquid. Dow Corning '200' series silicone oil, viscosity 200 cS, conductivity $3{\cdot}7 \times 10^{-4}$ c.g.s., depth 2·0 cm. (*a*) 'Rolls' in a square geometry, $\Delta T = 0{\cdot}67$ °C, $\eta = 0$. (*b*) Transition to two-dimensional rolls, $\Delta T = 1{\cdot}0$ °C, $\eta = 0$. (*c*) Transition to two-dimensional rolls, $\Delta T = 0{\cdot}63$ °C, $\eta = 0$.